Computational and Applied Mathematics (2023) 42:5
https://doi.org/10.1007/s40314-022-02144-2

An energy-stable second-order finite element method for the Swift–Hohenberg equation

Longzhao Qi[1] · **Yanren Hou**[1]

Received: 8 April 2022 / Revised: 17 November 2022 / Accepted: 27 November 2022

Abstract
In this paper, we design and analyze an unconditionally energy-stable, second-order-in-time, finite element scheme for the Swift–Hohenberg equation. We prove rigorously that our scheme is unconditionally uniquely solvable and unconditionally energy stable. We also give the boundedness of discrete phase variable for any time and space mesh sizes. Numerical tests are presented to validate the accuracy and energy stability of our scheme.

Keywords Swift–Hohenberg equation · Finite element · Energy stability · Boundedness

Mathematics Subject Classification 65M12 · 65M22 · 65M60

1 Introduction

The Swift–Hohenberg (SH) equation was originally introduced by Swift and Hohenberg to study the effects of thermal fluctuations on the Rayleigh–Bénard instability (Swift and Hohenberg 1977). It is an L^2-gradient flow for the following free energy functional (or Lyapunov functional)

$$\begin{aligned} E_1(u) &= \int_\Omega \left(\frac{1}{4}u^4 - \frac{\epsilon}{2}u^2 + \frac{1}{2}u(1+\Delta)^2 u \right) \mathrm{d}x \\ &= \int_\Omega \left(\frac{1}{4}(u^2-\epsilon)^2 + \frac{1}{2}u(1+\Delta)^2 u \right) \mathrm{d}x - \frac{\epsilon^2}{4}|\Omega|, \end{aligned} \tag{1.1}$$

where $|\Omega|$ is the measure of the convex polygonal domain Ω.

Communicated by Frederic Valentin.

Subsidized by National Natural Science Foundation of China (NSFC) (Grant No.11971378).

✉ Yanren Hou
yrhou@mail.xjtu.edu.cn

Longzhao Qi
15548367422@163.com

1 School of Mathematics and Statistics, Xi'an Jiaotong University, Xi'an 710049, People's Republic of China

Published online: 12 December 2022

The SH equation is given by

$$\partial_t u = -\omega, \qquad \text{in } \Omega \times (0, T], \tag{1.2}$$

$$\omega = u^3 - \epsilon u + (1+\Delta)\mu, \qquad \text{in } \Omega \times (0, T], \tag{1.3}$$

$$\mu = (1+\Delta)u, \qquad \text{in } \Omega \times (0, T], \tag{1.4}$$

$$u(x, 0) = u_0(x), \qquad \text{in } \Omega, \tag{1.5}$$

$$\partial_n u = \partial_n \omega = \partial_n \mu = 0, \qquad \text{on } \partial\Omega \times (0, T]. \tag{1.6}$$

where $\partial_t u = \frac{\partial u}{\partial t}$, u is the density field and $0 < \epsilon < 1$ is a constant with physical significance, Δ is the Laplace operator.

Taking the L^2-inner product of (1.2) with ω, we have

$$(\partial_t u, \omega) = -\|\omega\|^2. \tag{1.7}$$

Taking the L^2-inner product of (1.3) with $\partial_t u$, we get

$$(\omega, \partial_t u) = (u^3 - \epsilon u, \partial_t u) + ((1+\Delta)\mu, \partial_t u). \tag{1.8}$$

Differentiating both sides of (1.4) with respect to t, taking the L^2-inner product of the resulting equation with μ and using the homogeneous boundary condition (1.6), we have

$$(\mu_t, \mu) = ((1+\Delta)(\partial_t u), \mu) = (\partial_t u, (1+\Delta)\mu). \tag{1.9}$$

Combining (1.7–1.9), we obtain

$$\frac{\mathrm{d}}{\mathrm{d}t}\left(\int_\Omega \left[\frac{1}{4}u^4 - \frac{\epsilon}{2}u^2 + \frac{\epsilon^2}{4} + \frac{1}{2}\mu^2\right]\mathrm{d}x - \frac{\epsilon^2}{4}|\Omega|\right) = -\|\omega\|^2 \le 0. \tag{1.10}$$

Integrating (1.10) from 0 to t, we get the following energy dissipation law

$$E_2(u(t), \mu(t)) + \int_0^t \|\omega(s)\|^2 \mathrm{d}s = E_2(u_0, \mu_0),$$

where $\mu_0 = (1+\Delta)u_0$ and

$$E_2(u, \mu) = \int_\Omega \left(\frac{1}{4}(u^2 - \epsilon)^2 + \frac{1}{2}\mu^2\right)\mathrm{d}x - \frac{\epsilon^2}{4}|\Omega|. \tag{1.11}$$

Since $\mu = (1+\Delta)u$, the energy functional can also be written as

$$\begin{aligned} E_1(u) &= \int_\Omega \left[\frac{1}{4}(u^2 - \epsilon)^2 + \frac{1}{2}((1+\Delta)u)^2\right]\mathrm{d}x - \frac{\epsilon^2}{4}|\Omega| \\ &= \frac{1}{4}\|u^2 - \epsilon\|^2 + \frac{1}{2}\|(1+\Delta)u\|^2 - \frac{\epsilon^2}{4}|\Omega|. \end{aligned}$$

The H^{-1}-gradient flow of (1.1) is the phase field crystal (PFC) equation. The Swift–Hohenberg equation is the non-conserved counterpart of the PFC equation. This relationship is similar to that between the Allen–Cahn model and the Cahn–Hilliard model. As a nonlinear fourth-order partial differential equation, it is difficult to solve the SH equation analytically. Hence, efficient and accurate numerical schemes are necessary in studying of nonequilibrium processing. The main difficulty is associated with how to discrete the nonlinear term properly and preserve the energy stability. As we all know, the standard forward Euler scheme is unstable if time step τ exceeds a threshold proportional to h^4, where h is grid size. Recent years, several computational methods have been given to alleviate the restriction. A semi-implicit first-order finite difference scheme was presented in Cheng and James (2008), in which the authors divide the linear parts into forward and backward pieces and treat the nonlinear part explicitly. In Elsey and Wirth (2013), a first-order semi-implicit method was proposed, in which the authors insert an additional stabilizing term to improve the energy stability while keeping the simplicity. By applying the Crank–Nicolson scheme, a semi-implicit second-order method was given in Gomez and Nogueira (2012), in which the Newton's method was applied to solve the nonlinear equation at every time marching, but the optimal convergence analysis for that scheme was not discussed. In Lee (2017), by applying the operator splitting scheme, the first- and second-order Fourier spectral methods were presented to solve the SH equation; however, the error analysis and theoretical proof of the long time energy stability were not discussed. In Qi and Hou (2021), the authors proposed a second-order energy-stable numerical scheme for the SH equation and presented an optimal error estimate for the scheme. In Qi and Hou (2022d), the authors proposed a stabilized linear predictor-corrector scheme for the SH equation, they also proved rigorously that the scheme satisfies the energy dissipation law and is second-order accurate. In Qi and Hou (2022b), a stabilized linear Crank–Nicolson scheme for the SH equation was proposed and analyzed. In Qi and Hou (2022a), the authors presented first-and second-order energy-stable linear schemes for the Swift–Hohenberg equation based on first-order backward Euler and Crank–Nicolson schemes, respectively, a spectral-Galerkin approximation was adopted for the spatial variables and error estimate was established for the fully discrete second-order Crank–Nicolson scheme. For the SH system with quadratic-cubic nonlinear term, a first-order and second-order accurate schemes were presented in Lee (2019), in which the Fourier spectral method was applied for the spatial discretization. In Zhang and Ma (2016), by using the finite difference method, a large time-stepping scheme was given and analyzed for the SH equation. In Lee (2020), a new mass conservative SH equation was introduced and its first-order and second-order mass conservative operator splitting schemes were proposed, the authors also presented several numerical experiments to demonstrate the effectiveness of his methods, but he did not discuss convergence or error analysis. In Dehghan et al. (2022), the C^0-virtual element method was formulated and analyzed to solve generalized Swift–Hohenberg equation on polygonal meshes, and a priori error estimates and corresponding rates of convergence for the numerical solution were obtained. The direct meshless local Petrov–Galerkin (DMLPG) method was employed to solve the stochastic Cahn–Hilliard–Cook and Swift–Hohenberg equations in Abbaszadeh et al. (2019), in order to obtain a fully discrete scheme the direct meshless local collocation method was used to discretize the spatial variable and the Euler–Maruyama method was used for time discretization. In Dehghan and Abbaszadeh (2017), the authors considered a linear combination of shape functions of local radial basis functions collocation method and moving Kriging interpolation technique and designed the meshless local collocation method for solving multi-dimensional Cahn–Hilliard, Swift–Hohenberg and phase field crystal equations. In Dehghan et al. (2019), a reduced order discontinuous Galerkin method was developed for solving the generalized Swift–Hohenberg equation with application in biological science and mechanical engineering. There also have extensive works of convergent and energy-stable numerical methods for the PFC model (Wise et al. 2009; Hu et al. 2009; Elsey and Wirth 2013; Li and Kim 2017), the modified phase field crystal (MPFC) model (Wang and Wise 2011; Baskaran et al. 2013a, b; Qi and Hou 2023) and the square phase field crystal (SPFC) model (Cheng et al. 2019), treating the nonlinear terms implicitly, such as the convex splitting methods (Hu et al. 2009; Baskaran et al. 2013b; Elsey and Wirth 2013). The first-order and second-order accurate convex splitting methods (Hu et al. 2009; Baskaran et al. 2013b; Elsey and Wirth 2013), the finite difference methods (Hu et al. 2009; Wise et al. 2009; Wang and Wise 2011; Baskaran et al. 2013a; Li and Kim

2017) and Fourier pseudo-spectral methods (Zhai et al. 2021; Yang and Han 2017), the 2D and 3D numerical results (Li and Kim 2017; Yang and Han 2017), have been widely reported.

In this paper, we give a new fully discrete finite element scheme for the SH equation in the mixed formulation based on Crank–Nicolson scheme. Instead of the standard Crank–Nicolson scheme, we use the diffusive Crank–Nicolson scheme, that is, replacing $(1+\Delta)(u^{n+1}+u^n)/2$ with $(1+\Delta)(3u^{n+1}+u^{n-1})/4$ to approximate $(1+\Delta)u(t_{n+1/2})$. We observe in Qi and Hou (2022c) that one shortcoming of the standard Crank–Nicolson scheme is that the uniqueness of the numerical solution requires that the time step τ satisfies the condition $0<\tau\le 2/\epsilon$. The diffusive Crank–Nicolson scheme enjoys all the advantages of the standard Crank–Nicolson scheme and satisfies unconditionally unique solvability. We also prove unconditional energy stability for this scheme. Numerical results are given to validate the energy stability and accuracy of our numerical scheme.

The rest of the paper is organized as follows. In Sect. 2, we give the fully discrete finite element scheme for the SH equation in the mixed formulation and prove the unconditionally unique solvability and the energy stability, In Sect. 3, numerical tests are presented to validate the accuracy and energy stability. Finally, we conclude the paper in Sect. 4.

2 The second-order finite element scheme in the mixed formulation

The weak formulation of (1.2–1.6) can be written as follows: find (u,ω,μ) such that

$$u\in L^\infty(0,T;H^1(\Omega))\cap L^4(0,T;L^\infty(\Omega)),\ \ \omega,\mu\in L^2(0,T;H^1(\Omega)),$$

and for almost all $t\in(0,T]$, there holds

$$(\partial_t u,\varphi)=-(\omega,\varphi),\ \ \forall\,\varphi\in H^1(\Omega), \tag{2.1}$$

$$(\omega,\psi)=(u^3,\psi)-\epsilon(u,\psi)+((1+\Delta)\mu,\psi),\ \ \forall\,\psi\in H^1(\Omega), \tag{2.2}$$

$$(\mu,\zeta)=((1+\Delta)u,\zeta),\ \ \forall\,\zeta\in H^1(\Omega). \tag{2.3}$$

Let N be a positive integer and $0=t_0<t_1<\cdots<t_N=T$ be a uniform partition of $[0,T]$ with $\tau=t_i-t_{i-1}$ and $i=1,\ldots,N$. Suppose $\mathcal{T}_h=\{K\}$ is a quasi-uniform, shape-regular, conforming family of triangulations of Ω. For $q\in\mathbb{Z}^+$, define $V_h:=\{v\in\mathcal{C}(\Omega)\mid v|_K\in\mathcal{P}_q(K),\forall\,K\in\mathcal{T}_h\}\subset H^1(\Omega)$, where $\mathcal{P}_q$ denotes the polynomials space with the degree not greater than q. The second-order finite element scheme in the mixed formulation is defined as follows: for any $1\le n\le N-1$, given $u_h^n,u_h^{n-1}\in V_h$, find $u_h^{n+1},\omega_h^{n+1/2},\mu_h^{n+1/2}\in V_h$ such that

$$(\delta_\tau u_h^{n+1/2},\varphi)+(\omega_h^{n+1/2},\varphi)=0,\ \ \forall\,\varphi\in V_h, \tag{2.4}$$

$$(\omega_h^{n+1/2},\psi)=(\Lambda(u_h^{n+1},u_h^n),\psi)-\epsilon(\tilde{u}_h^{n+1/2},\psi)+((1+\Delta_h)\check{\mu}_h^{n+1/2},\psi),\ \ \forall\,\psi\in V_h, \tag{2.5}$$

$$(\check{\mu}_h^{n+1/2},\zeta)=((1+\Delta_h)\check{u}_h^{n+1/2},\zeta),\ \ \forall\,\zeta\in V_h, \tag{2.6}$$

where

$$\delta_\tau u_h^{n+1/2}:=\frac{u_h^{n+1}-u_h^n}{\tau},\ \ u_h^{n+1/2}:=\frac{1}{2}u_h^{n+1}+\frac{1}{2}u_h^n,\ \ \tilde{u}_h^{n+1/2}:=\frac{3}{2}u_h^n-\frac{1}{2}u_h^{n-1},$$
$$\check{u}_h^{n+1/2}:=\frac{3}{4}u_h^{n+1}+\frac{1}{4}u_h^{n-1},\ \ \Lambda(u_h^{n+1},u_h^n):=\frac{1}{2}((u_h^{n+1})^2+(u_h^n)^2)u_h^{n+1/2},$$

$$\check{\mu}_h^{n+1/2} := \frac{3}{4}\mu_h^{n+1} + \frac{1}{4}\mu_h^{n-1},\ \forall\, n \geq 1,\ \ \mu_h^n := (1+\Delta_h)u_h^n,\ \forall\, n \geq 0.$$

The discrete Laplacian $\Delta_h : V_h \to V_h$ is defined as follows: for any $v_h \in V_h$, $\Delta_h v_h \in V_h$ denotes the unique solution to the problem

$$(\Delta_h v_h, \xi) = -(\nabla v_h, \nabla \xi),\ \ \forall\, \xi \in V_h. \tag{2.7}$$

(2.4–2.6) is a multi-step scheme and it requires a separate initialization process. For the first step, the scheme is as follows: given $u_h^0 \in V_h$, find $u_h^1, \omega_h^{1/2}, \mu_h^{1/2} \in V_h$ such that

$$(\delta_\tau u_h^{1/2}, \varphi) + (\omega_h^{1/2}, \varphi) = 0,\ \forall\, \varphi \in V_h, \tag{2.8}$$

$$(\omega_h^{1/2}, \psi) = (\Lambda(u_h^1, u_h^0), \psi) - \epsilon(u_h^0, \psi) + \epsilon\frac{\tau}{2}(\omega_h^0, \psi) + ((1+\Delta_h)\mu_h^{1/2}, \psi),\ \forall\, \psi \in V_h, \tag{2.9}$$

$$(\mu_h^{1/2}, \zeta) = ((1+\Delta_h)u_h^{1/2}, \zeta),\ \forall\, \zeta \in V_h. \tag{2.10}$$

Since

$$\left(u_h^0 + \frac{\tau}{2}\partial_t u_h^0, \psi\right) = (u_h^0, \psi) + \frac{\tau}{2}(\partial_t u_h^0, \psi) = (u_h^0, \psi) - \frac{\tau}{2}(\omega_h^0, \psi),$$

we use $(u_h^0, \psi) - \frac{\tau}{2}(\omega_h^0, \psi)$ to approximate $(u_h^{1/2}, \psi)$ in (2.9). The scheme requires initial data $\omega_h^0 \in V_h$, which is defined as $\omega_h^0 = R_h\omega^0$ and

$$\omega^0 := u_0^3 - \epsilon u_0 + (1+\Delta)^2 u_0,$$

where $u_h^0 := R_h u_0$ and $R_h : H^1(\Omega) \to V_h$ is a standard Ritz projection:

$$(\nabla(R_h u - u), \nabla\xi) = 0,\ \forall\, \xi \in V_h,\ \ (R_h u - u, 1) = 0. \tag{2.11}$$

We also define the L^2 projection $P_h : L^2(\Omega) \to V_h$ as

$$(P_h u - u, \xi) = 0,\ \ \forall\, \xi \in V_h. \tag{2.12}$$

Theorem 2.1 *The fully discrete schemes (2.4–2.6) and (2.8–2.10) have a unique solution.*

Proof Taking the test function as $\zeta = (1+\Delta_h)\varphi$ in (2.6), we obtain

$$(\check{\mu}_h^{n+1/2}, (1+\Delta_h)\varphi) = ((1+\Delta_h)\check{u}_h^{n+1/2}, (1+\Delta_h)\varphi).$$

Moreover,

$$(\check{\mu}_h^{n+1/2}, (1+\Delta_h)\varphi) = ((1+\Delta_h)\check{\mu}_h^{n+1/2}, \varphi),$$

we have

$$((1+\Delta_h)\check{\mu}_h^{n+1/2}, \varphi) = ((1+\Delta_h)\check{u}_h^{n+1/2}, (1+\Delta_h)\varphi). \tag{2.13}$$

Taking the test function as $\psi = \varphi \in V_h$ in (2.5) and combing the resulting equation with (2.4) and (2.13), we get

$$(\delta_\tau u_h^{n+1/2}, \varphi) + (\Lambda(u_h^{n+1}, u_h^n), \varphi) - \epsilon(\tilde{u}_h^{n+1/2}, \varphi) + ((1+\Delta_h)\check{u}_h^{n+1/2}, (1+\Delta_h)\varphi) = 0,$$

that is

$$\left(\frac{u_h^{n+1}-u_h^n}{\tau},\varphi\right)+\left(\frac{(u_h^{n+1})^3+(u_h^{n+1})^2u_h^n+u_h^{n+1}(u_h^n)^2+(u_h^n)^3}{4},\varphi\right)$$
$$-\epsilon\left(\frac{3}{2}u_h^n-\frac{1}{2}u_h^{n-1},\varphi\right)+\left(\frac{3}{4}(1+\Delta_h)u_h^{n+1}+\frac{1}{4}(1+\Delta_h)u_h^{n-1},(1+\Delta_h)\varphi\right)=0.$$

By rearranging the above equation, we get for every $\varphi\in V_h$,

$$\frac{1}{\tau}(u_h^{n+1},\varphi)+\frac{1}{4}((u_h^{n+1})^3+(u_h^{n+1})^2u_h^n+u_h^{n+1}(u_h^n)^2,\varphi)$$
$$+\frac{3}{4}((1+\Delta_h)u_h^{n+1},(1+\Delta_h)\varphi)=f[u_h^n,u_h^{n-1}](\varphi), \tag{2.14}$$

where $f[u_h^n,u_h^{n-1}]$ is a bounded linear functional involving the previous time iteration. Based on the scheme (2.14), we define the following functional:

$$J(u_h)=\frac{1}{2\tau}\int_\Omega(u_h)^2\mathrm{d}x+\frac{1}{4}\int_\Omega\left[\frac{1}{4}(u_h)^4+\frac{1}{3}(u_h)^3u_h^n+\frac{1}{2}(u_h)^2(u_h^n)^2\right]\mathrm{d}x$$
$$+\frac{3}{8}\int_\Omega((1+\Delta_h)u_h)^2\mathrm{d}x-f[u_h^n,u_h^{n-1}](u_h).$$

It may be shown that u_h^{n+1} is the unique minimizer of $J(u_h)$ if and only if it solves, for any φ,

$$\frac{\mathrm{d}}{\mathrm{d}s}J(u_h+s\varphi)\mid_{s=0}=\frac{1}{\tau}(u_h,\varphi)+\frac{1}{4}((u_h)^3+(u_h)^2u_h^n+u_h(u_h^n)^2,\varphi)$$
$$+\frac{3}{4}((1+\Delta_h)u_h,(1+\Delta_h)\varphi)-f[u_h^n,u_h^{n-1}](\varphi)=0.$$

Since

$$\begin{aligned}\frac{\mathrm{d}^2}{\mathrm{d}s^2}J(u_h+s\varphi)\mid_{s=0}&=\frac{1}{\tau}\int_\Omega\varphi^2\mathrm{d}x+\frac{1}{4}\int_\Omega\left[3(u_h)^2\varphi^2+2u_hu_h^n\varphi^2+(u_h^n)^2\varphi^2\right]\mathrm{d}x\\&\quad+\frac{3}{4}\int_\Omega((1+\Delta_h)\varphi)^2\mathrm{d}x\\&=\frac{1}{\tau}\int_\Omega\varphi^2\mathrm{d}x+\frac{1}{4}\int_\Omega\left[2(u_h)^2\varphi^2+((u_h)^2+2u_hu_h^n+(u_h^n)^2)\varphi^2\right]\mathrm{d}x\\&\quad+\frac{3}{4}\int_\Omega((1+\Delta_h)\varphi)^2\mathrm{d}x\\&\geq0,\end{aligned}$$

the corresponding functional $J(u_h)$ is a convex functional and the uniqueness of the solution of scheme (2.4–2.6) is proved. The unique solvability of the initialization scheme (2.8–2.10) can be proved similarly. □

Theorem 2.2 *Let $(u_h^1,\omega_h^{1/2},\mu_h^{1/2})\in V_h\times V_h\times V_h$ be the solution of the initialization scheme (2.8–2.10). Then, the first-step energy dissipation law holds for any $h,\tau>0$:*

$$E_2(u_h^1,\mu_h^1)+\tau\|\omega_h^{1/2}\|^2+\frac{\epsilon}{4}\|u_h^1-u_h^0\|^2\leq E_2(u_h^0,\mu_h^0)+\frac{\epsilon\tau^2}{4}\|\omega_h^0\|^2, \tag{2.15}$$

where $E_2(u,\mu)$ is defined in (1.11).

Proof Setting $\varphi = \tau\omega_h^{1/2}$ in (2.8), $\psi = \tau\delta_\tau u_h^{1/2} = u_h^1 - u_h^0$ in (2.9) and $\zeta = (1+\Delta_h)(u_h^1 - u_h^0)$ in (2.10), we get

$$\tau(\delta_\tau u_h^{1/2}, \omega_h^{1/2}) + \tau\|\omega_h^{1/2}\|^2 = 0, \tag{2.16}$$

$$\begin{aligned}(\omega_h^{1/2}, u_h^1 - u_h^0) &= (\Lambda(u_h^1, u_h^0), u_h^1 - u_h^0) - \epsilon(u_h^0, u_h^1 - u^0) \\ &\quad + \epsilon\frac{\tau}{2}(\omega_h^0, u_h^1 - u_h^0) + ((1+\Delta_h)\mu_h^{1/2}, u_h^1 - u_h^0),\end{aligned} \tag{2.17}$$

$$\begin{aligned}(\mu_h^{1/2}, (1+\Delta_h)(u_h^1 - u_h^0)) &= ((1+\Delta_h)u_h^{1/2}, (1+\Delta_h)(u_h^1 - u_h^0)) \\ &= \frac{1}{2}(\|(1+\Delta_h)u_h^1\|^2 - \|(1+\Delta_h)u_h^0\|^2).\end{aligned} \tag{2.18}$$

Note that

$$(\Lambda(u_h^1, u_h^0), u_h^1 - u_h^0) = \frac{1}{4}(\|u_h^1\|_{L^4}^4 - \|u_h^0\|_{L^4}^4), \tag{2.19}$$

$$\epsilon(u_h^0, u_h^1 - u_h^0) = \frac{\epsilon}{2}(\|u_h^1\|^2 - \|u_h^0\|^2 - \|u_h^1 - u_h^0\|^2), \tag{2.20}$$

$$((1+\Delta_h)\mu_h^{1/2}, u_h^1 - u_h^0) = (\mu_h^{1/2}, (1+\Delta_h)(u_h^1 - u_h^0)). \tag{2.21}$$

Combining (2.16–2.18), we have

$$\begin{aligned}&\frac{1}{4}(\|u_h^1\|_{L^4}^4 - \|u_h^0\|_{L^4}^4) - \frac{\epsilon}{2}(\|u_h^1\|^2 - \|u_h^0\|^2) + \frac{\epsilon}{2}\|u_h^1 - u_h^0\|^2 \\ &+ \frac{1}{2}(\|(1+\Delta_h)u_h^1\|^2 - \|(1+\Delta_h)u_h^0\|^2) \\ = &-\tau\|\omega_h^{1/2}\|^2 - \epsilon\frac{\tau}{2}(\omega_h^0, u_h^1 - u_h^0) \\ \leq &-\tau\|\omega_h^{1/2}\|^2 + \frac{\epsilon\tau^2}{4}\|\omega_h^0\|^2 + \frac{\epsilon}{4}\|u_h^1 - u_h^0\|^2,\end{aligned}$$

that is,

$$\begin{aligned}&\frac{1}{4}(\|u_h^1\|_{L^4}^4 - \|u_h^0\|_{L^4}^4) - \frac{\epsilon}{2}(\|u_h^1\|^2 - \|u_h^0\|^2) + \frac{\epsilon}{4}\|u_h^1 - u_h^0\|^2 \\ &+ \frac{1}{2}(\|(1+\Delta_h)u_h^1\|^2 - \|(1+\Delta_h)u_h^0\|^2) \leq -\tau\|\omega_h^{1/2}\|^2 + \frac{\epsilon\tau^2}{4}\|\omega_h^0\|^2,\end{aligned}$$

which is the desired result. □

Next, we define a modified energy functional:

$$F(u, v) := E_1(u) + \frac{\epsilon}{4}\|u - v\|^2 + \frac{1}{8}\|(1+\Delta_h)(u - v)\|^2. \tag{2.22}$$

Theorem 2.3 *Let* $(u_h^{n+1}, \omega_h^{n+1/2}, \mu_h^{n+1/2}) \in V_h \times V_h \times V_h$ *be the solution of (2.4–2.6) and* $(u_h^1, \omega_h^{1/2}, \mu_h^{1/2}) \in V_h \times V_h \times V_h$ *be the solution of (2.8–2.10). Then, the following energy dissipation law holds for any* $h, \tau > 0$*:*

$$
\begin{aligned}
&F(u_h^{l+1}, u_h^l) + \tau \sum_{n=1}^{l} \|\omega_h^{n+1/2}\|^2 \\
&\quad + \sum_{n=1}^{l} \left[\frac{\epsilon}{4} \|u_h^{n+1} - 2u_h^n + u_h^{n-1}\|^2 + \frac{1}{8} \|(1+\Delta_h)(u_h^{n+1} - 2u_h^n + u_h^{n-1})\|^2 \right] \\
&\quad = F(u_h^1, u_h^0), \quad \forall\, 1 \le l \le N-1.
\end{aligned} \tag{2.23}
$$

Proof Setting $\varphi = \omega_h^{n+1/2}$ in (2.4), $\psi = \delta_\tau u_h^{n+1/2}$ in (2.5) and $\zeta = (1+\Delta_h)\delta_\tau u_h^{n+1/2}$ in (2.6), we have

$$
(\delta_\tau u_h^{n+1/2}, \omega_h^{n+1/2}) + \|\omega_h^{n+1/2}\|^2 = 0, \tag{2.24}
$$

$$
\begin{aligned}
&(\omega_h^{n+1/2}, \delta_\tau u_h^{n+1/2}) = (\Lambda(u_h^{n+1}, u_h^n), \delta_\tau u_h^{n+1/2}) \\
&- \epsilon(\tilde{u}_h^{n+1/2}, \delta_\tau u_h^{n+1/2}) + ((1+\Delta_h)\breve{\mu}_h^{n+1/2}, \delta_\tau u_h^{n+1/2}),
\end{aligned} \tag{2.25}
$$

$$
(\breve{\mu}_h^{n+1/2}, (1+\Delta_h)\delta_\tau u_h^{n+1/2}) = ((1+\Delta_h)\breve{u}_h^{n+1/2}, (1+\Delta_h)\delta_\tau u_h^{n+1/2}). \tag{2.26}
$$

Note that

$$
\begin{aligned}
&(\Lambda(u_h^{n+1}, u_h^n), \delta_\tau u_h^{n+1/2}) \\
&\quad = \frac{1}{4\tau}(\|u_h^{n+1}\|_{L^4}^4 - \|u_h^n\|_{L^4}^4), \\
&\quad - \epsilon(\tilde{u}_h^{n+1/2}, \delta_\tau u_h^{n+1/2}) = -\epsilon(\frac{3}{2}u_h^n - \frac{1}{2}u_h^{n-1}, \frac{1}{\tau}(u_h^{n+1} - u_h^n)) \\
&\quad = -\frac{\epsilon}{2\tau}(\|u_h^{n+1}\|^2 - \|u_h^n\|^2) + \frac{\epsilon}{4\tau}\|u_h^{n+1} - u_h^n\|^2 - \frac{\epsilon}{4\tau}\|u_h^n - u_h^{n-1}\|^2 \\
&\quad + \frac{\epsilon}{4\tau}\|u_h^{n+1} - 2u_h^n + u_h^n\|^2, \\
&\quad ((1+\Delta_h)\breve{u}_h^{n+1/2}, (1+\Delta_h)\delta_\tau u_h^{n+1/2}) = \frac{1}{2\tau}(\|(1+\Delta_h)u_h^{n+1}\|^2 - \|(1+\Delta_h)u_h^n\|) \\
&\quad + \frac{1}{8\tau}(\|(1+\Delta_h)(u_h^{n+1} - u_h^n)\|^2 - \|(1+\Delta_h)(u_h^n - u_h^{n-1})\|^2) \\
&\quad + \frac{1}{8\tau}\|(1+\Delta_h)(u_h^{n+1} - 2u_h^n + u_h^{n-1})\|^2.
\end{aligned}
$$

Combining (2.24–2.26), we have

$$
\begin{aligned}
-\|\omega_h^{n+1/2}\|^2 &= \frac{1}{4\tau}(\|u_h^{n+1}\|_{L^4}^4 - \|u_h^n\|_{L^4}^4) - \frac{\epsilon}{2\tau}(\|u_h^{n+1}\|^2 - \|u_h^n\|^2) \\
&\quad + \frac{\epsilon}{4\tau}\|u_h^{n+1} - u_h^n\|^2 - \frac{\epsilon}{4\tau}\|u_h^n - u_h^{n-1}\|^2 + \frac{\epsilon}{4\tau}\|u_h^{n+1} - 2u_h^n + u_h^{n-1}\|^2 \\
&\quad + \frac{1}{2\tau}\|(1+\Delta_h)u_h^{n+1}\|^2 - \frac{1}{2\tau}\|(1+\Delta_h)u_h^n\|^2 + \frac{1}{8\tau}\|(1+\Delta_h)(u_h^{n+1} - u_h^n)\|^2 \\
&\quad - \frac{1}{8\tau}\|(1+\Delta_h)(u_h^n - u_h^{n-1})\|^2 + \frac{1}{8\tau}\|(1+\Delta_h)(u_h^{n+1} - 2u_h^n + u_h^{n-1})\|^2,
\end{aligned}
$$

that is,

$$
\begin{aligned}
&\frac{1}{\tau}F(u_h^{n+1}, u_h^n) - \frac{1}{\tau}F(u_h^n, u_h^{n-1}) + \frac{\epsilon}{4\tau}\|u_h^{n+1} - 2u_h^n + u_h^{n-1}\|^2 \\
&\qquad + \frac{1}{8\tau}\|(1+\Delta_h)(u_h^{n+1} - 2u_h^n + u_h^{n-1})\|^2 + \|\omega_h^{n+1/2}\|^2 = 0.
\end{aligned} \tag{2.27}
$$

Applying the operator $\tau \sum_{n=1}^{l}$ to equation (2.27), we obtain the desired result. □

Throughout this paper, we shall denote a generic positive constant by the letter C and at its different occurrences, it may stand for different values. In this work, we assume that the initial data satisfies the following stability:

$$E_2(u_h^0, \mu_h^0) + \tau^2 \|\omega_h^0\|^2 + \|\Delta_h u_h^0\|^2 \leq C, \tag{2.28}$$

where $\mu_h^0 := R_h \mu_0$.

Theorem 2.4 *Let $(u_h^{n+1}, \omega_h^{n+1/2}, \mu_h^{n+1/2}) \in V_h \times V_h \times V_h$ be the solution of (2.4–2.6) and $(u_h^1, \omega_h^{1/2}, \mu_h^{1/2}) \in V_h \times V_h \times V_h$ be the solution of (2.8–2.10). We have the following estimates for any $h, \tau > 0$:*

$$\max_{0 \leq n \leq N} \left[\|(1+\Delta_h) u_h^n\|^2 + \|(u_h^n)^2 - \epsilon\|^2 \right] \leq C, \tag{2.29}$$

$$\max_{0 \leq n \leq N} \left[\|u_h^n\|_{L^4}^4 + \|u_h^n\|^2 + \|\nabla u_h^n\|^2 + \|\Delta_h u_h^n\|^2 \right] \leq C, \tag{2.30}$$

$$\max_{1 \leq n \leq N} \left[\|u_h^n - u_h^{n-1}\|^2 + \|(1+\Delta_h)(u_h^n - u_h^{n-1})\|^2 \right] \leq C, \tag{2.31}$$

$$\tau \sum_{n=0}^{N-1} \|\omega_h^{n+1/2}\|^2 \leq C, \tag{2.32}$$

$$\sum_{n=1}^{N-1} \left[\|u_h^{n+1} - 2u_h^n + u_h^{n-1}\|^2 + \|(1+\Delta_h)(u_h^{n+1} - 2u_h^n + u_h^{n-1})\|^2 \right] \leq C, \tag{2.33}$$

for some positive constant C which is independent of h, τ and T.

Proof From (2.15) and (2.28), we get

$$\begin{aligned}
&\|u_h^0\|_{L^4}^4 = \|(u_h^0)^2\|^2 = \|(u_h^0)^2 - \epsilon + \epsilon\|^2 \leq 2\|(u_h^0)^2 - \epsilon\|^2 + 2\|\epsilon\|^2 \leq C, \\
&\|(u_h^1)^2 - \epsilon\|^2 + \|(1+\Delta_h) u_h^1\|^2 + \tau \|\omega_h^{1/2}\|^2 + \|u_h^1 - u_h^0\|^2 \leq C.
\end{aligned}$$

Hence, we have

$$\begin{aligned}
&\|u_h^1\|_{L^4}^4 = \|(u_h^1)^2\|^2 = \|(u_h^1)^2 - \epsilon + \epsilon\|^2 \leq 2\|(u_h^1)^2 - \epsilon\|^2 + 2\|\epsilon\|^2 \leq C, \\
&\|u_h^0\|^2 = \|(1+\Delta_h) u_h^0 - \Delta_h u_h^0\|^2 \leq 2\|(1+\Delta_h) u_h^0\|^2 + 2\|\Delta_h u_h^0\|^2 \leq C, \\
&\|u_h^1\|^2 = \|(u_h^1 - u_h^0) + u_h^0\|^2 \leq 2\|u_h^1 - u_h^0\|^2 + 2\|u_h^0\|^2 \leq C, \\
&\|\Delta_h u_h^1\| = \|(1+\Delta_h) u_h^1 - u_h^1\| \leq \|(1+\Delta_h) u_h^1\| + \|u_h^1\| \leq C, \\
&\|\nabla u_h^1\|^2 = (\nabla u_h^1, \nabla u_h^1) = |(u_h^1, \Delta_h u_h^1)| \leq \frac{1}{2}\|u_h^1\|^2 + \frac{1}{2}\|\Delta_h u_h^1\|^2 \leq C
\end{aligned}$$

Using the triangle inequality, we get

$$F(u_h^1, u_h^0) = E_1(u_h^1) + \frac{\epsilon}{4}\|u_h^1 - u_h^0\|^2 + \frac{1}{8}\|(1+\Delta_h)(u_h^1 - u_h^0)\|^2 \leq C. \tag{2.34}$$

Combining (2.23), (2.34) and the fact that $E_1(u_h^{n+1}) \leq F(u_h^{n+1}, u_h^n)$, for $0 \leq n \leq N-1$, using the approach as above, we can obtain all of the inequalities. □

Next, we give a priori estimates. We first introduce some results about H^{-1}-norm given in Diegel et al. (2015). Let $L_0^2(\Omega)$ be the set of functions in $L^2(\Omega)$ with zero mean, we set

$$\mathring{H}^1 = H^1(\Omega) \cap L_0^2(\Omega), \quad \mathring{H}^{-1} := \{\phi \in H^{-1}(\Omega) \mid (v, 1) = 0\}.$$

We define $\mathbb{T} : \mathring{H}^{-1}(\Omega) \to \mathring{H}^1(\Omega)$ as follow: given $u \in \mathring{H}^{-1}(\Omega)$, find $\mathbb{T}(u) \in \mathring{H}^1(\Omega)$ such that

$$(\nabla \mathbb{T}(u), \nabla v) = (u, v), \quad \forall\, v \in \mathring{H}^1(\Omega).$$

Let $u, v \in \mathring{H}^{-1}(\Omega)$ and set

$$(u, v)_{H^{-1}} := (\nabla \mathbb{T}(u), \nabla \mathbb{T}(v)) = (u, \mathbb{T}(v)) = (\mathbb{T}(u), v),$$

$(\cdot, \cdot)_{H^{-1}}$ defines an inner product on $\mathring{H}^{-1}(\Omega)$, the induced norm is equal to the operator norm:

$$\|u\|_{H^{-1}} := \sqrt{(u, u)_{H^{-1}}} = \sup_{0 \neq v \in \mathring{H}^1(\Omega)} \frac{(u, v)}{\|\nabla v\|}. \tag{2.35}$$

Consequently, for all $v \in H^1(\Omega)$ and all $u \in \mathring{H}^{-1}(\Omega)$,

$$|(u, v)| \leq \|u\|_{H^{-1}} \|\nabla v\|.$$

Moreover, for all $v \in L_0^2(\Omega)$, we have the Poincaré-type inequality

$$\|u\|_{H^{-1}} \leq C\|u\|,$$

where $C > 0$ is the Poincaré constant.

Let $\mathring{V}_h = V_h \cap L_0^2(\Omega)$. The corresponding discrete operator $\mathbb{T}_h : \mathring{V}_h \to \mathring{V}_h$ can be defined as follows: given $u \in \mathring{V}_h$, find $\mathbb{T}_h(u) \in \mathring{V}_h$ such that

$$(\nabla \mathbb{T}_h(u), \nabla v) = (u, v), \quad \forall v \in \mathring{V}_h.$$

Let $u, v \in \mathring{V}_h$ and set

$$(u, v)_{-1,h} := (\nabla \mathbb{T}_h(u), \nabla \mathbb{T}_h(v)) = (u, \mathbb{T}_h(v)) = (\mathbb{T}_h(u), v),$$

$(\cdot, \cdot)_{-1,h}$ defines an inner product on $\mathring{V}_h$, the induced norm satisfies

$$\|u\|_{-1,h} := \sqrt{(u, u)_{-1,h}} = \sup_{0 \neq v \in \mathring{V}_h} \frac{(u, v)}{\|\nabla v\|}.$$

Consequently, for all $v \in \mathring{V}_h$ and $u \in \mathring{V}_h$,

$$|(u, v)| \leq \|u\|_{-1,h} \|\nabla v\|.$$

The following Poincaré-type estimate holds

$$\|u\|_{-1,h} \leq C\|u\|, \quad \forall u \in \mathring{V}_h,$$

for some $C > 0$ that is independent of h.

Before further investigation, we introduce the following discrete Gagliardo–Nirenberg inequality and its proof is referred to Page 21–Page 23 in Diegel (2015).

Lemma 2.1 (Discrete Gagliardo–Nirenberg inequality) *Suppose $\mathcal{T}_h$ is a conforming mesh (no hanging nodes) that is globally quasi-uniform and Ω is a convex polygonal domain. For all $v \in V_h$, there is a constant $C > 0$ such that for $d = 2, 3$,*

$$\|v_h\|_{L^\infty} \leq C\|\Delta_h v_h\|_{L^2}^{\frac{d}{2(6-d)}} \|v_h\|_{L^6}^{\frac{3(4-d)}{2(6-d)}} + C\|u_h\|_{L^6},$$

where Δ_h is the discrete Laplace operator.

Theorem 2.5 *Let $(u_h^{n+1}, \omega_h^{n+1/2}, \mu_h^{n+1/2}) \in V_h \times V_h \times V_h$ be the solution of (2.4–2.6) and $(u_h^1, \omega_h^{1/2}, \mu_h^{1/2}) \in V_h \times V_h \times V_h$ be the solution of (2.8–2.10). Then, we have the following estimates hold for any $h, \tau > 0$:*

$$\tau \sum_{n=0}^{N-1} \left[\|\delta_\tau u_h^{n+1/2}\|_{H^{-1}}^2 + \|\delta_\tau u_h^{n+1/2}\|_{-1,h}^2 + \|\delta_\tau u_h^{n+1/2}\|^2\right] \leq C, \tag{2.36}$$

$$\tau \sum_{n=0}^{N-1} \left[\|(1+\Delta_h)\check{u}_h^{n+1/2}\|^2 + \|\check{u}_h^{n+1/2}\|_{L^\infty}^{4(6-d)/d}\right] \leq C. \tag{2.37}$$

Proof Choose $\varphi \in H_0^1(\Omega)$, by (2.4) and (2.8), for all $0 < n < N-1$,

$$\begin{aligned}(\delta_\tau u_h^{n+1/2}, \varphi) = (\delta_\tau u_h^{n+1/2}, P_h\varphi) &= -(\omega_h^{n+1/2}, P_h\varphi) \\ &\leq \|\omega_h^{n+1/2}\|\|P_h\varphi\| \leq C\|\omega_h^{n+1/2}\|\|\varphi\|,\end{aligned} \tag{2.38}$$

where P_h is defined in (2.12) and the H^1-stability of the L^2-projection is used in the last step. Using (2.32), we have $\|\omega_h^{n+1/2}\| \leq C$, hence $(\delta_\tau u_h^{n+1/2}, \varphi) \leq C\|\varphi\|$ and using the definition of H^{-1}-norm (2.35), we get

$$\|\delta_\tau u_h^{n+1/2}\| = \sup_{0\neq\varphi\in \mathring{H}_0^1} \frac{(\delta_\tau u_h^{n+1/2}, \varphi)}{\|\varphi\|} \leq C,$$

$$\|\delta_\tau u_h^{n+1/2}\|_{H^{-1}} = \sup_{0\neq\varphi\in \mathring{H}_0^1} \frac{(\delta_\tau u_h^{n+1/2}, \varphi)}{\|\nabla\varphi\|} \leq \sup_{0\neq\varphi\in \mathring{H}_0^1} \frac{(\delta_\tau u_h^{n+1/2}, \varphi)}{C\|\varphi\|} \leq C,$$

where the Poincaré inequality is used. From the inequality $\|\phi\|_{-1,h} \leq \|\phi\|_{H^{-1}}, \forall\, \phi \in V_h$, we obtain (2.36).

Setting $\psi = \check{u}_h^{n+1/2}$ in (2.5) and $\zeta = (1+\Delta_h)\check{u}_h^{n+1/2}$ in (2.6), we have for all $1 \leq n \leq N-1$,

$$\begin{aligned}\|(1+\Delta_h)\check{u}_h^{n+1/2}\|^2 &= (\check{\mu}_h^{n+1/2}, (1+\Delta_h)\check{u}_h^{n+1/2}) = ((1+\Delta_h)\check{\mu}_h^{n+1/2}, \check{u}_h^{n+1/2}) \\ &= (\omega_h^{n+1/2}, \check{u}_h^{n+1/2}) + \epsilon(\tilde{u}_h^{n+1/2}, \check{u}_h^{n+1/2}) - (\Lambda(u_h^{n+1}, u_h^n), \check{u}_h^{n+1/2}) \\ &\leq \|\omega_h^{n+1/2}\|^2 + \frac{1}{4}\|\check{u}_h^{n+1/2}\|^2 + \frac{\epsilon^2}{2}\|\tilde{u}_h^{n+1/2}\|^2 + \frac{1}{2}\|\check{u}_h^{n+1/2}\|^2 \\ &\quad + \frac{1}{2}\|\Lambda(u_h^{n+1}, u_h^n)\|^2 + \frac{1}{2}\|\check{u}_h^{n+1/2}\|^2 \\ &= \|\omega_h^{n+1/2}\|^2 + \frac{\epsilon^2}{2}\|\tilde{u}_h^{n+1/2}\|^2 + \frac{1}{2}\|\Lambda(u_h^{n+1}, u_h^n)\|^2 + \frac{5}{4}\|\check{u}_h^{n+1/2}\|^2.\end{aligned} \tag{2.39}$$

Applying Lemma 2.4, we get the following estimates for all $0 \le n \le N-1$,

$$\begin{aligned}\|\Lambda(u_h^{n+1}, u_h^n)\|^2 = &\frac{1}{16}\|(u_h^{n+1})^3 + (u_h^{n+1})^2 u_h^n + u_h^{n+1}(u_h^n)^2 + (u_h^n)^3\|^2\\ \le& C\|(u_h^{n+1})^3\|^2 + C\|(u_h^{n+1})^2 u_h^n\|^2 + C\|u_h^{n+1}(u_h^n)^2\|^2 + C\|(u_h^n)^3\|^2\\ \le& C\|u_h^{n+1}\|\|u_h^{n+1}\|_{L^4}^2 + C\|u_h^n\|\|u_h^{n+1}\|_{L^4}^2 + C\|u_h^{n+1}\|\|u_h^n\|_{L^4}^2\\ &+ C\|u_h^n\|\|u_h^n\|_{L^4}^2\\ \le& C.\end{aligned} \tag{2.40}$$

$$\|\tilde{u}_h^{n+1/2}\|^2 = \|\frac{3}{2}u_h^n - \frac{1}{2}u_h^{n-1}\|^2 \le C(\|u_h^n\|^2 + \|u_h^{n-1}\|^2) \le C. \tag{2.41}$$

$$\|\check{u}_h^{n+1/2}\|^2 = \|\frac{3}{4}u_h^{n+1} + \frac{1}{4}u_h^{n-1}\|^2 \le C(\|u_h^{n+1}\|^2 + \|u_h^{n-1}\|^2) \le C. \tag{2.42}$$

Combining (2.39–2.42), we have

$$\|(1+\Delta_h)\check{u}_h^{n+1/2}\|^2 \le \|\omega_h^{n+1/2}\|^2 + C.$$

Applying $\tau\sum_{n=0}^{N-1}$ and using (2.32), we obtain the first estimate of (2.37).

To derive the second estimate of (2.37), we apply the discrete Gagliardo–Nirenberg inequality:

$$\|\phi_h^n\|_{L^\infty} \le C\|\Delta_h\phi_h^n\|^{d/2(6-d)}\|\phi_h^n\|_{L^6}^{3(4-d)/2(6-d)} + C\|\phi_h^n\|_{L^6}, \quad \forall\, \phi_h^n \in V_h, \ (d=2,3) \tag{2.43}$$

Using (2.42) and the first estimate of (2.37), we have

$$\|\Delta_h\check{u}_h^{n+1/2}\| = \|(1+\Delta_h)\check{u}_h^{n+1/2} - \check{u}_h^{n+1/2}\| \le \|(1+\Delta_h)\check{u}_h^{n+1/2}\| + \|\check{u}_h^{n+1/2}\| \le C, \tag{2.44}$$

$$\begin{aligned}\|\nabla\check{u}_h^{n+1/2}\|^2 &= (\nabla\check{u}_h^{n+1/2}, \nabla\check{u}_h^{n+1/2}) = |(\check{u}_h^{n+1/2}, \Delta_h\check{u}_h^{n+1/2})|\\ &\le \frac{1}{2}\|\check{u}_h^{n+1/2}\|^2 + \frac{1}{2}\|\Delta_h\check{u}_h^{n+1/2}\|^2 \le C,\end{aligned} \tag{2.45}$$

Applying $\tau\sum_{n=1}^{N-1}$ and using $H^1(\Omega) \hookrightarrow L^6(\Omega)$, (2.44) and (2.45), we get the second estimate of (2.37). □

3 Numerical experiments

3.1 Convergence and energy stability test

We first give some numerical experiments to validate the convergence rate of our scheme. We take $\Omega = (0,1)^2$, $\epsilon = 0.025$. We choose a source term to the equation such that the analytical solution is given by

$$u(x, y, t) = e^{-t}\cos(\pi x)\cos(2\pi x).$$

Both $\mathcal{P}_1$ and $\mathcal{P}_2$ elements are chosen in the spatial discretization.

We first test the spatial convergence rate. We choose the spatial meshes with different size $h = 1/4, 1/8, 1/16, 1/32, 1/64$. The time step size should be set small enough so

Table 1 The errors and the convergence rates at $T = 1.0E - 7$ for the phase field variable u with distinct spatial mesh size. The time step size is $\tau = 1.0E - 9$ and the parameter is $\epsilon = 0.025$

	h	L^2 error	Rate		h	L^2 error	Rate
$\mathcal{P}_1$ element	1/4	1.36900E−1	–	$\mathcal{P}_2$ element	1/4	1.38266E−2	–
	1/8	3.69585E−2	1.88914		1/8	1.74597E−3	2.98535
	1/16	9.42272E−3	1.97169		1/16	2.24973E−4	2.95620
	1/32	2.36872E−3	1.99204		1/32	2.87496E−5	2.96814
	1/64	5.93714E−4	1.99627		1/64	3.82117E−6	2.91145

Table 2 The errors and the convergence rates at $T = 1.0E - 7$ for the phase field variable u with distinct spatial mesh size. The time step size is $\tau = 1.0E - 9$ and the parameter is $\epsilon = 0.1$

	h	L^2 error	Rate		h	L^2 error	Rate
$\mathcal{P}_1$ element	1/4	1.36854E−1	–	$\mathcal{P}_2$ element	1/4	1.37954E−2	–
	1/8	3.68965E−2	1.89108		1/8	1.75698E−3	2.97302
	1/16	9.42369E−3	1.96912		1/16	2.25469E−4	2.96210
	1/32	2.36795E−3	1.99265		1/32	2.88954E−5	2.96402
	1/64	5.94856E−4	1.99303		1/64	3.83649E−6	2.91298

Table 3 The errors and the convergence rates at $T = 1.0E - 7$ for the phase field variable u with distinct spatial mesh size. The time step size is $\tau = 1.0E - 9$ and the parameter is $\epsilon = 0.25$

	h	L^2 error	Rate		h	L^2 error	Rate
$\mathcal{P}_1$ element	1/4	1.37454E−1	–	$\mathcal{P}_2$ element	1/4	1.37945E−2	–
	1/8	3.68923E−2	1.89756		1/8	1.75692E−3	2.97297
	1/16	9.43648E−3	1.96700		1/16	2.25649E−4	2.96090
	1/32	2.37822E−3	1.98837		1/32	2.88974E−5	2.96507
	1/64	5.94613E−4	1.99986		1/64	3.81546E−6	2.92101

that, compared with the spatial error, the temporal error is negligible. Hence, we choose $\tau = 1 \times 10^{-9}$ and $T = 1 \times 10^{-7}$. The L^2-errors between the numerical solution and the analytical solution are given in Table 1-Table 3 with distinct parameter ϵ, which validates the optimal error estimate of $\mathcal{P}_1$ and $\mathcal{P}_2$ elements. We then test the temporal convergence rate. We set $2h = \tau = 2/4$, 2/8, 2/16, 2/32, 2/64 and the final time is $T = 2$. The result is listed in Table 4-Table 6 with distinct parameter ϵ, which shows our scheme is second-order-in-time.

We now test the evolution of energy functional of the numerical solution. We choose the initial condition as follows:

$$u(x, y) = \sin\left(\frac{\pi x}{16}\right)\cos\left(\frac{\pi y}{16}\right).$$

We take $\Omega = (0, 32)^2$, $\epsilon = 0.025$, $h = 1/4$, $T = 10$. Figure 1a gives the energy evolution with respect to different time step size τ, which shows that our scheme satisfies unconditional energy stability. Figure 1b shows that the energy decay is robust with respect to the physical parameter ϵ.

Table 4 The errors and the convergence rates at $T = 2$ for the phase field variable u with distinct time step size. The spatial mesh size is $h = \tau/2$ and the parameter is $\epsilon = 0.025$

	τ	L^2 error	Rate		τ	L^2 error	Rate
$\mathcal{P}_1$ element	2/4	4.21346E−2	–	$\mathcal{P}_2$ element	2/4	3.63853E−3	–
	2/8	1.42864E−2	1.56036		2/8	4.52135E−4	3.00853
	2/16	3.87536E−3	1.88224		2/16	6.83953E−5	2.72478
	2/32	9.92244E−4	1.96556		2/32	1.31435E−5	2.37955
	2/64	2.49743E−4	1.99025		2/64	2.97224E−6	2.14473

Table 5 The errors and the convergence rates at $T = 2$ for the phase field variable u with distinct time step size. The spatial mesh size is $h = \tau/2$ and the parameter is $\epsilon = 0.1$

	τ	L^2 error	Rate		τ	L^2 error	Rate
$\mathcal{P}_1$ element	2/4	4.22648E−2	–	$\mathcal{P}_2$ element	2/4	3.64955E−3	–
	2/8	1.43649E−2	1.55691		2/8	4.53648E−4	3.00807
	2/16	3.88496E−3	1.88658		2/16	6.84613E−5	2.72821
	2/32	9.93159E−4	1.96780		2/32	1.32348E−5	2.37095
	2/64	2.50495E−4	1.98724		2/64	2.98946E−6	2.14638

Table 6 The errors and the convergence rates at $T = 2$ for the phase field variable u with distinct time step size. The spatial mesh size is $h = \tau/2$ and the parameter is $\epsilon = 0.25$

	τ	L^2 error	Rate		τ	L^2 error	Rate
$\mathcal{P}_1$ element	2/4	4.20546E−2	–	$\mathcal{P}_2$ element	2/4	3.62964E−3	–
	2/8	1.41495E−2	1.57151		2/8	4.51642E−4	3.00657
	2/16	3.86976E−3	1.87044		2/16	6.82976E−5	2.72527
	2/32	9.91359E−4	1.96476		2/32	1.30349E−5	2.38946
	2/64	2.48942E−4	1.99360		2/64	2.96975E−6	2.13397

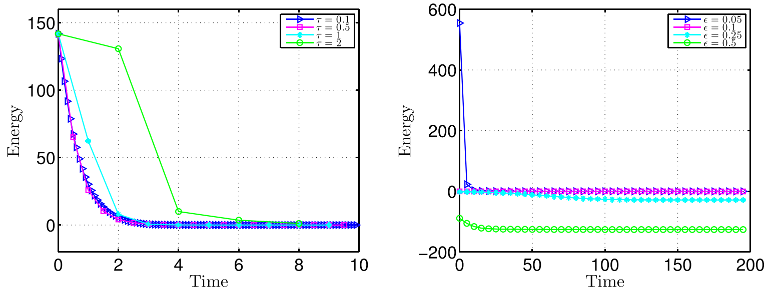

(a) (b)

Fig. 1 Energy evolution diagrams with distinct time step size τ (**a**) and distinct physical parameter ϵ (**b**)

3.2 Phase transition behaviors

3.2.1 Time evolution of random perturbation

We choose the randomly perturbed initial condition as follows

$$u(x, y, 0) = 0.2 + 0.02\text{rand}(x, y),$$

where rand is a randomly chosen number between -1 and 1 at the grid points. The computational domain is $(-20, 20) \times (-20, 20)$. Let the spatial grid size be $h = 1/4$, the time step be $\tau = 1$, $\epsilon = 0.025$. Figure 2 shows that our scheme does lead to the expected states. Figure 3 displays the results at $t = 100$ with respect to four different values of ϵ, i.e., ϵ= 0.05, 0.1, 0.25 and 0.5 with domain $(-30, 30) \times (-30, 30)$. We can find that a large value of ϵ accelerates the formation of regular laminar pattern.

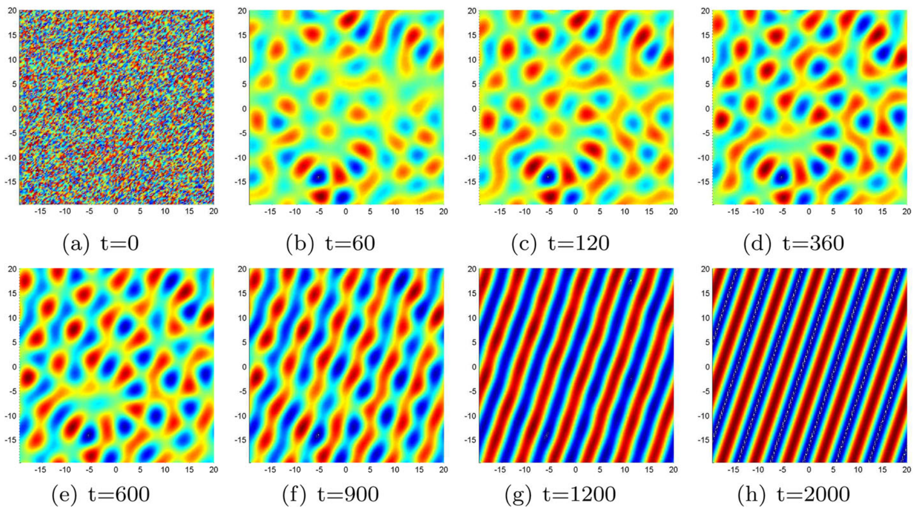

Fig. 2 The evolution of the phase transition behavior. Snapshots of the numerical approximation of the phase variable u are taken at $t = 0, 60, 120, 360, 600, 900, 1200, 2000$. The computational domain is $(-20, 20) \times (-20, 20)$. The parameters are $\epsilon = 0.025$, $\tau = 1$, $h = 1/4$, $T = 2000$

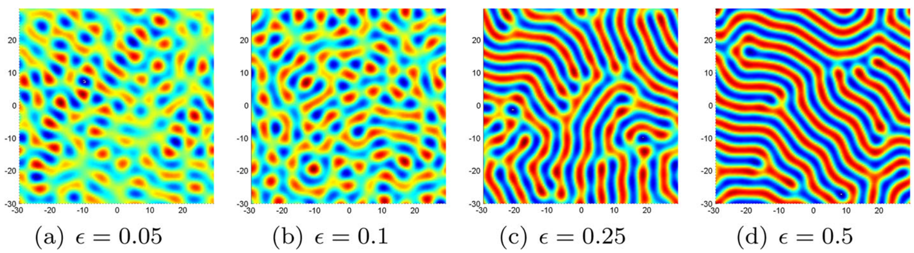

Fig. 3 Snapshots at $t = 100$ with respect to different values of ϵ

3.2.2 2D crystal growth in a supercooled liquid

The crystal growth in a supercooled liquid was considered as an important benchmark test in two-dimensional space. Here, we consider the growth of one crystal nucleus with the following initial condition:

$$u(x, y, 0) = 0.14 + \alpha \text{rand}(x, y),$$

where α takes the value of $\alpha = 1$ for the crystal nucleus locating at (90, 90). The diameter of the nucleus is 4. The computational domain is the circle domain with center (90, 90) and radius 90. $h = 2$, $\tau = 1/2$, $\epsilon = 0.45$ and $T = 100$. Figure 4 shows the growth of the nuclei in time. Figure 5 shows the energy evolution of the 2D crystal growth in a supercooled liquid.

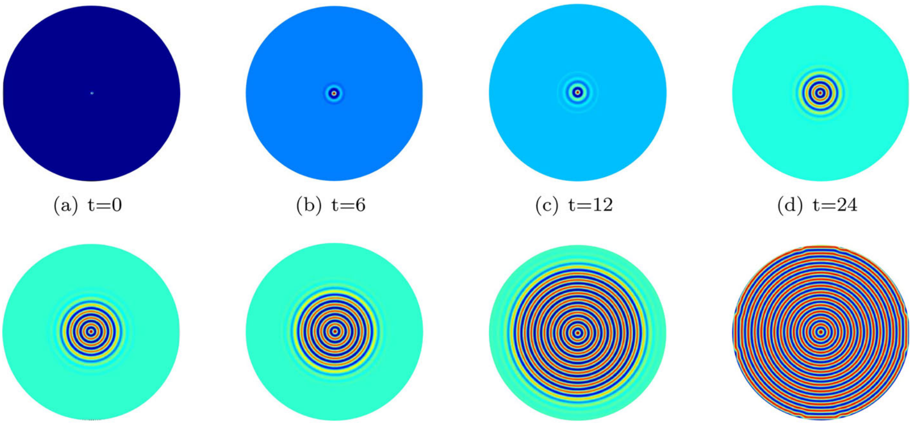

(a) t=0 (b) t=6 (c) t=12 (d) t=24

(e) t=32 (f) t=40 (g) t=60 (h) t=100

Fig. 4 Temporal evolution of 2D crystal growth in a supercooled liquid. The parameters are $\epsilon = 0.45$, $\tau = 1/2$, $h = 2$, $T = 100$

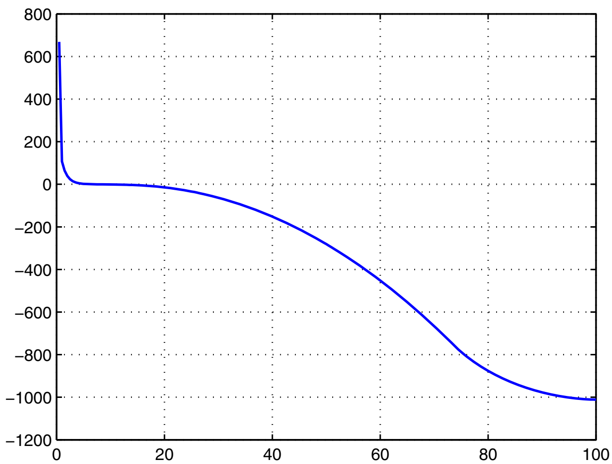

Fig. 5 The energy evolution of the 2D crystal growth in a supercooled liquid

4 Conclusions

In this work, an unconditionally energy-stable, second-order finite element scheme in the mixed formulation is given and analyzed for the SH equation. The unconditionally unique solvability and energy stability are rigorously proved. We also give the boundedness of the discrete phase variable for any time and space mesh sizes. Finally, numerical test is presented to validate the accuracy and energy stability of the proposed numerical strategy.

Acknowledgements This work was supported by the National Natural Science Foundation of China (NSFC) (No. 11971378).

Data Availability No data was used for the research described in the article.

Declarations

Conflicts of Interests The authors declared that they have no conflicts of interest to this work.

References

Abbaszadeh M, Khodadadian A, Parvizi M, Dehghan M, Heitzinger C (2019) A direct meshless local collocation method for solving stochastic Cahn–Hilliard–Cook and stochastic Swift–Hohenberg equations. Eng Anal Boundary Elem 98:253–264. https://doi.org/10.1016/j.enganabound.2018.10.021

Baskaran A, Hu Z, Lowengrub JS, Wang C, Wise SM, Zhou P (2013) Energy stable and efficient finite-difference nonlinear multigrid schemes for the modified phase field crystal equation. J Comput Phys 250:270–292

Baskaran A, Lowengrub JS, Wang C, Wise SM (2013) Convergence analysis of a second order convex splitting scheme for the modified phase field crystal equation. SIAM J Numer Anal 51(5):2851–2873. https://doi.org/10.1137/120880677

Cheng K, Wang C, Wise SM (2019) An energy stable BDF2 Fourier pseudo-spectral numerical scheme for the square phase field crystal equation. Commun Comput Phys 26(5):1335–1364

Cheng M, James AW (2008) An efficient algorithm for solving the phase field crystal model. J Comput Phys 227(12):6241–6248. https://doi.org/10.1016/j.jcp.2008.03.012

Dehghan M, Abbaszadeh M (2017) The meshless local collocation method for solving multi-dimensional Cahn–Hilliard, Swift–Hohenberg and phase field crystal equations. Eng Anal Boundary Elem 78:49–64. https://doi.org/10.1016/j.enganabound.2017.02.005

Dehghan M, Abbaszadeh M, Khodadadian A, Heitzinger C (2019) Galerkin proper orthogonal decomposition-reduced order method (POD-ROM) for solving generalized Swift–Hohenberg equation. Int J Numer Meth Heat Fluid Flow 29(8):2642–2665. https://doi.org/10.1108/HFF-11-2018-0647

Dehghan M, Gharibi Z, Eslahchi MR (2022) Unconditionally energy stable C0-virtual element scheme for solving generalized Swift–Hohenberg equation. Appl Numer Math 178:304–328. https://doi.org/10.1016/j.apnum.2022.03.013

Diegel AE (2015) Numerical analysis of convex splitting schemes for Cahn-Hilliard and coupled Cahn-Hilliard-fluid-flow equations. *Ph.D. Thesis*, University of Tennessee

Diegel AE, Feng XH, Wise SM (2015) Analysis of a mixed finite element method for a Cahn–Hilliard–Darcy–Stokes system. SIAM J Numer Anal 53(1):127–152

Elsey M, Wirth B (2013) A simple and efficient scheme for phase field crystal simulation. ESAIM Math Model Numer Anal 47(5):1413–1432

Gomez H, Nogueira X (2012) A new space-time discretization for the Swift–Hohenberg equation that strictly respects the Lyapunov functional. Commun Nonlinear Sci Numer Simul 17(12):4930–4946

Hu Z, Wise SM, Wang C, Lowengrub JS (2009) Stable and efficient finite-difference nonlinear-multigrid schemes for the phase field crystal equation. J Comput Phys 228(15):5323–5339

Lee HG (2017) A semi-analytical Fourier spectral method for the Swift–Hohenberg equation. Comput Math Appl 74(8):1885–1896

Lee HG (2019) An energy stable method for the Swift-Hohenberg equation with quadratic-cubic nonlinearity. Comput Methods Appl Mech Eng 343:40–51

Lee HG (2020) A new conservative Swift–Hohenberg equation and its mass conservative method. J Comput Appl Math 375:112815. https://doi.org/10.1016/j.cam.2020.112815

Li Y, Kim J (2017) An efficient and stable compact fourth-order finite difference scheme for the phase field crystal equation. Comput Methods Appl Mech Eng 319:194–216. https://doi.org/10.1016/j.cma.2017.02.022

Qi L, Hou Y (2021) A second order energy stable BDF numerical scheme for the Swift–Hohenberg equation. J Sci Comput 88(3):1–25

Qi L, Hou Y (2022) Error analysis of first- and second-order linear, unconditionally energy-stable schemes for the Swift–Hohenberg equation. Comput Math Appl 127:192–212. https://doi.org/10.1016/j.camwa.2022.10.007

Qi L, Hou Y (2022) An unconditionally energy-stable linear Crank–Nicolson scheme for the Swift–Hohenberg equation. Appl Numer Math 181:46–58. https://doi.org/10.1016/j.apnum.2022.05.018

Qi L, Hou Y (2022c) Numerical analysis of a second-order mixed finite element method for the Swift-Hohenberg equation. *preprint*

Qi L, Hou Y (2022) Error estimate of a stabilized second-order linear predictor-corrector scheme for the Swift-Hohenberg equation. Appl Math Lett 127:107836

Qi L, Hou Y (2023) Error estimates for the Scalar Auxiliary Variable (SAV) schemes to the modified phase field crystal equation. J Comput Appl Math 417:114579. https://doi.org/10.1016/j.cam.2022.114579

Swift JB, Hohenberg PC (1977) Hydrodynamic fluctuations at the convective instability. Phys Rev A 15(1):319–328

Wang C, Wise SM (2011) An energy stable and convergent finite-difference scheme for the modified phase field crystal equation. SIAM J Numer Anal 49(3):945–969. https://doi.org/10.1137/090752675

Wise SM, Wang C, Lowengrub JS (2009) An energy-stable and convergent finite-difference scheme for the phase field crystal equation. SIAM J Numer Anal 47(3):2269–2288. https://doi.org/10.1137/080738143

Yang X, Han D (2017) Linearly first- and second-order, unconditionally energy stable schemes for the phase field crystal model. J Comput Phys 330:1116–1134

Zhai S, Weng Z, Feng X, He Y (2021) Stability and error estimate of the operator splitting method for the phase field crystal equation. J Sci Comput 86:1

Zhang Z, Ma Y (2016) On a large time-stepping method for the Swift-Hohenberg equation. Adv Appl Math Mech 8(6):992–1003